ACADEMIC PRESS

Available online at www.sciencedirect.com
SCIENCE DIRECT®

NeuroImage

NeuroImage 20 (2003) 257–264

www.elsevier.com/locate/ynimg

Functional brain imaging of olfactory processing in monkeys

J.M. Boyett-Anderson,[a] D.M. Lyons,[a] A.L. Reiss,[a,b,c] A.F. Schatzberg,[a,c] and V. Menon[a,b,c,*]

[a] *Department of Psychiatry and Behavioral Sciences, Stanford University, Stanford, CA 94305, USA*
[b] *Program in Neuroscience, Stanford University, Stanford, CA 94305, USA*
[c] *Stanford Brain Research Institute, Stanford University, Stanford, CA 94305, USA*

Received 7 October 2002; revised 12 May 2003; accepted 20 May 2003

Abstract

As a step toward bridging the gap between human and animal studies of olfactory brain systems, we report results from an fMRI study of olfaction in squirrel monkeys. High-resolution fMRI images at 3 T with $1.25 \times 1.25 \times 1.2$ mm^3 voxels were obtained covering the whole brain using an 8-cm-diameter birdcage coil and a gradient–echo spiral pulse sequence. Data were acquired from six sedated adult males using a standard block design. All fMRI data were spatially normalized to a common template and analyzed at the individual and group levels with statistical parametric and nonparametric methods. Robust odorant-induced activations were detected in several brain regions previously implicated in conscious human olfactory processing, including the orbitofrontal cortex, cerebellum, and piriform cortex. Consistent with human data, no stimulus intensity effects were observed in any of these regions. Average signal changes in these regions exceeded 0.6%, more than three times the expected signal change based on human fMRI studies of olfaction adjusting for differences in voxel size. These results demonstrate the feasibility of studying olfaction in sedated monkeys with imaging techniques commonly used at 3 T in humans and help promote direct comparisons between humans and nonhuman primates. Our findings, for example, provide novel support for the hypothesis that the cerebellum is involved in sensory acquisition. More broadly, this study suggests that olfactory processing in sedated monkeys and nonsedated humans shares similar neural substrates both within and beyond the primary olfactory system.

Keywords: fMRI; Olfaction; Orbitofrontal cortex; Cerebellum; Squirrel monkey; Sedation; Consciousness

Introduction

Current understanding of olfactory neural processing comes primarily from electrophysiological, anatomical, biochemical, and lesion studies in animals (Doty, 2001; Hildebrand and Shepherd, 1997; Kauer and White, 2001; Shipley and Ennis, 1996) and brain lesion studies in humans (West and Doty, 1995). Such studies have elucidated the involvement of the olfactory bulb, piriform cortex, and entorhinal cortex in olfaction. Recently, this picture of olfactory processing has been broadened by imaging studies designed to explore the linked neural substrates of olfaction in alert conscious humans.

The first positron emission tomography (PET) studies in the early 1990s (Zatorre and Jones-Gotman, 1991; Zatorre et al., 1992) paved the way for later work using single photon emission tomography (SPECT) (Malaspina et al., 1998) and high-resolution functional magnetic resonance imaging (fMRI) (Anderson et al., 2003; Sobel et al., 1998a, 1997, 1999). These studies of human olfaction have discerned the involvement of the piriform and entorhinal cortices, as well as other brain regions that play less obvious functional roles, i.e., orbitofrontal cortex and the cerebellum. Despite the striking complementarity of the human and animal literature, no single research modality has been used to tie together the region-specific findings from electrophysiological, neuroanatomical, biochemical, and lesion studies in animals with the more global picture emerging from imaging studies of humans.

Here we report fMRI techniques for investigating olfac-

* Corresponding author. Program in Neuroscience and Department of Psychiatry and Behavioral Sciences, 401 Quarry Rd., Stanford, CA 94305-5719.

E-mail address: menon@stanford.edu (V. Menon).

1053-8119/03/$ – see front matter © 2003 Elsevier Inc. All rights reserved.
doi:10.1016/S1053-8119(03)00288-X

tion in sedated squirrel monkeys. fMRI studies of olfactory processing have typically examined alert conscious humans (Zald and Pardo, 2000). A significant body of evidence, however, indicates that processes such as classical conditioning with olfactory cues occur in sedated animals (Lovibond and Shanks, 2002). The neural substrates of olfactory processing during sedation are largely unknown, but fMRI studies of animals have compared the extent and intensity of brain activation elicited by sensory stimulation in sedated and nonsedated states (Lahti et al., 1999; Leopold et al., 2002). Although sedation appears to dampen blood oxygenation level-dependent (BOLD) intensities in visual and somatosensory regions (Ferris et al., 2001; Lahti et al., 1999; Leopold et al., 2002; Plettenberg et al., 2002), sedation effects are variable across different regions of brain (Sparks et al., 1973; Yang et al., 1998). Olfactory brain systems in rodents, for example, apparently maintain robust activation in sedated and nonsedated states (Xu et al., 2000; Yang et al., 1998).

Previous fMRI studies of monkeys have focused on the visual system (Dubowitz et al., 1998; Leite et al., 2002; Logothetis et al., 2002, 1999; Stefanacci et al., 1998). Only one study thus far has examined olfaction in nonhuman primates (Ferris et al., 2001). Activations in the preoptic area and anterior hypothalamus of male marmoset monkeys were examined in response to a single presentation of a sexually relevant odor. fMRI data were not presented for the entire marmoset brain, and a single OFF–ON–OFF cycle of epochs was used, with each epoch of odorant presentation lasting 7–10 min. Neuroimaging studies of humans have demonstrated that four to six cycles are consistently required to accurately estimate the BOLD response (Moonen and Bandettini, 1999; Skudlarski et al., 1999). Moreover, long epochs often lead to confounds with low-frequency drift and result in suboptimal detection of task-related activation (Skudlarski et al., 1999).

The present study of olfaction in monkeys relied on a statistically valid experimental paradigm, homogenous in- and out-of-plane voxel dimensions, and rapid image acquisition using a 3T MRI scanner. Data were normalized to a common brain template for fixed-effects analysis at the individual and group levels using statistical parametric and nonparametric methods. The imaging and stimulus presentation parameters used here with monkeys are similar to those found in human fMRI studies and facilitate direct comparisons between human and monkey olfaction.

Methods

Subjects

Six adult male squirrel monkeys (*Saimiri sciureus*) that were born and raised under standard laboratory conditions at Stanford University served as subjects. All procedures were conducted in accord with and as required by the Animal Welfare Act and were approved by Stanford University's Administrative Panel on Laboratory Animal Care.

Immediately prior to each scan session, monkeys were sedated with a subcutaneous injection of 20 mg/kg of ketamine hydrochloride, 4 mg/kg of xylazine hydrochloride, and 0.04 mg/kg of atropine sulfate. Body temperatures were maintained within the normal range using a cushioned heat pad. Earplugs provided protection from noise generated by the scanner and taped cotton pads blocked all visual sources of sensory input.

Experimental design and procedures

Based on pilot tests, three concentrations of acetic acid odorant were selected and prepared in distilled water (1.0, 0.1, and 0.01% by volume). These concentrations were consistently rated by seven humans as being strong, mild, and barely detectable. Each of the six monkeys was tested with each odorant concentration in three successive experiments during a single 35 min session. Each experiment consisted of 10 40 s epochs which alternated between one odorant concentration and a no-odorant control condition (distilled water alone). Both odorant and no-odorant presentations were made with saturated cotton-tipped applicators placed 2–3 cm from the monkey's face. A continuous stream of oxygen flowing over the monkey promoted transitions between the odorant and no-odorant presentations. The order of presentation for each odorant concentration experiment was counterbalanced across the six subjects and included an undisturbed 3- 4 min interval between each of the three experiments.

fMRI scanning

All images were acquired on a 3T scanner (GE Signa, Echospeed v8.3) with a custom-built 8-cm-diameter birdcage coil used in both transmit and receive modes. The scanner runs on an LX platform, with gradients in "Mini-CRM" configuration (35 mT/m, SR 190 mT/m/s) and has a Magnex 3T 80 cm magnet. At the beginning of each session, a high-resolution series of T1-weighted anatomical images throughout the entire brain was acquired with a 3D inversion recovery prepared fast spoiled gradient recalled acquisition in steady-state (SPGR) pulse sequence: TR, 10 ms; TE, 2 ms; TI, 300 ms; flip angle, 15°; NEX, 2; field of view, 8 $\times$ 8 cm; data matrix, 256 $\times$ 256; voxel size, 0.312 $\times$ 0.312 $\times$ 1.20 mm for 24 contiguous slices. Functional brain images for each experiment were thereafter acquired in the identical spatial location and orientation with a gradient echo spiral pulse sequence: TR, 3000 ms; TE, 30 ms; flip angle, 70°; field of view, 8 $\times$ 8 cm; data matrix, 64 $\times$ 64; voxel size, 1.25 $\times$ 1.25 $\times$ 1.20 mm for 24 contiguous slices.

Data analysis

Images were reconstructed by inverse Fourier transformation for each time point. fMRI data were preprocessed using SPM99 (http://www.fil.ion.ucl.ac.uk/spm). Images were corrected for movement using least square minimization without higher order corrections for spin history. To facilitate group-level analyses, all fMRI scans were normalized to a common template. T2*-weighted images corresponding to the monkey with the best structural MRI data were selected as the template. The quality of realignment was visually inspected and found to result in very minor loss of resolution relative to the volumes of brain regions of interest (ROIs) specified below.

For each monkey, voxel-level comparisons of odorant versus no-odorant activation were determined separately for each odorant concentration using multivariate regression analysis with corrections for temporal autocorrelations (Friston et al., 1995). The confounding effects of global mean fluctuations were corrected by proportional scaling, and low-frequency noise was removed with a high-pass filter (0.5 cycles/min). A regressor waveform for each test condition, convolved with a gamma function accounting for delay and dispersion in the hemodynamic response, was used to compute voxelwise t statistics. These t scores were then normalized to Z scores. A height threshold of $Z > 3.09$ ($P < 0.001$) and an extent threshold of five voxels were used to identify significantly activated voxels for odorant versus no-odorant comparisons at the group level. Activations are shown superposed on the T1-weighted template images using MRIcro (Rorden and Brett, 2000).

The percentage of voxels activated above threshold ($Z > 1.67$, $P < 0.05$) in each ROI was computed separately for each monkey. Differences were examined as a function of odorant concentration and hemispheric lateralization using nonparametric Friedman's tests and Wilcox pairwise comparisons. Test statistics were assessed at $P < 0.05$, two-tailed.

From representative voxels in each ROI, time series data were extracted for the mid-level odorant concentration in the monkey that provided the common brain template. Power spectral densities were computed using Welch's averaged modified periodogram method of spectral estimation after applying a Hamming window (Hayes, 1996). Additional time series data were also extracted from each individual monkey for small voxel clusters (1.25 mm in diameter) centered on the group activation peak in each ROI. These time series data were used to calculate the percentage of signal change in a given ROI for each of the six monkey subjects. For each anatomically defined ROI, the average percentage of signal change was considered to differ significantly ($P < 0.05$) from chance when the lower 95% confidence interval boundary (two-tailed) was found to be greater than 0.

Anatomically defined ROIs

To examine region-specific patterns of activation, five ROIs were drawn on high-resolution anatomical images of the template brain. As shown in Fig. 1 (top), these five ROIs encompassed the orbitofrontal cortex, piriform cortex, entorhinal cortex, cerebellum, and hippocampus. ROIs were identified using landmarks specified in the squirrel monkey brain atlas (Gergen and MacLean, 1962), supplemented with information from a cynomologous macaque monkey brain atlas (Martin, 2000). Hippocampal and orbitofrontal cortex ROIs were demarcated as indicated elsewhere in detail (Lyons et al., 2002, 2001). The cerebellum was identified by its obvious gross boundaries as depicted in brain imaging studies of humans and nonhuman primates (Semendeferi and Damasio, 2000). This ROI included all gray and white matter cerebellar brain tissue. The entorhinal cortex was demarcated as gray matter tissue on each coronal section that contained the rhinal sulcus and amygdala–hippocampal complex. The entorhinal ROI was bounded medially and inferiorly by the outer brain surface, superiorly by temporal lobe white matter tissue, and laterally by a line through the rhinal sulcus to adjacent white matter. The piriform cortex was demarcated as gray matter tissue on coronal sections extending from the posterior orbit caudally to the optic chiasm. The piriform ROI was bounded inferiorly by the outer brain surface, laterally by a line from the inferior tip of the anterior external capsule to the outer inferior brain surface, and superiorly by a line interconnecting the left and right lateral Sylvian sulcus.

Results

Group-level activation

The distributed network of BOLD activations evoked by odorants in sedated squirrel monkeys included the orbitofrontal cortex, cerebellum, and, to a lesser extent, hippocampus and piriform cortices (Fig. 1, bottom). BOLD signal activation was not detected in the entorhinal cortex. This undoubtedly reflects the high susceptibility of this region to dropout artifacts. The entorhinal ROI was therefore excluded from from further analysis.

Increased BOLD signal intensities in representative voxels from olfactory brain regions were time-locked with the odorant presentations (Fig. 2, left). In the spectral analysis, clear peaks were discerned at the task frequency for olfactory regions, but not in the visual cortex, which served as a control region (Fig. 2, right). Overall, 1592, or 14.5%, of the voxels examined throughout the brain showed significant activation.

Group-level deactivation

Voxels that showed greater activation during clean air "resting" baseline compared to odorant presentations were also examined for evidence of odorant-induced "deactiva-

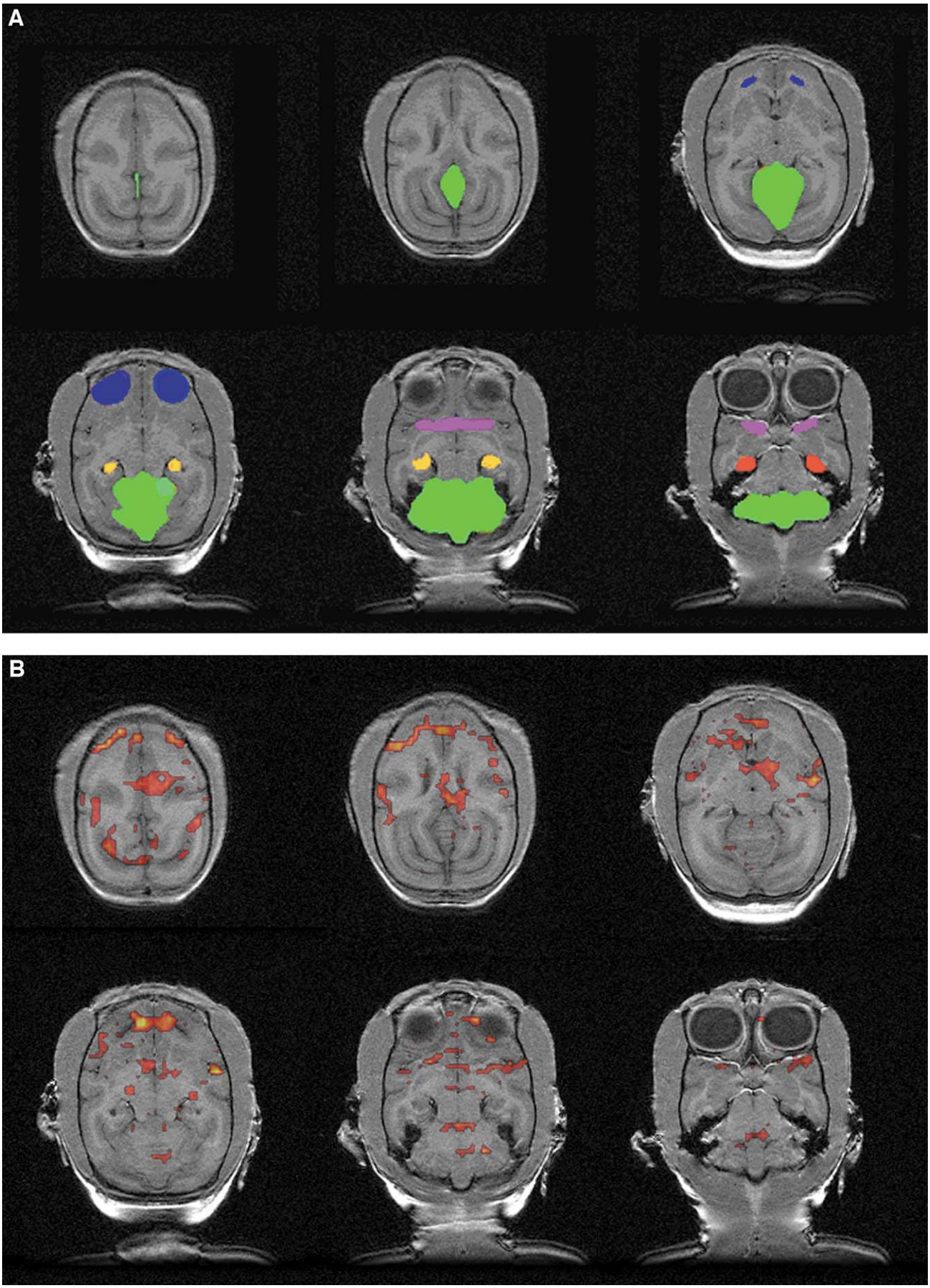

Fig. 1. (A) Regions of interest presented on the squirrel monkey brain template. Orbitofrontal cortex, blue; cerebellum, green; hippocampus, yellow; entorhinal cortex, red; piriform cortex, purple. (B) fMRI activation evoked by odorant presentation compared to clean air with a fixed-effects analysis depicted for six monkeys combined.

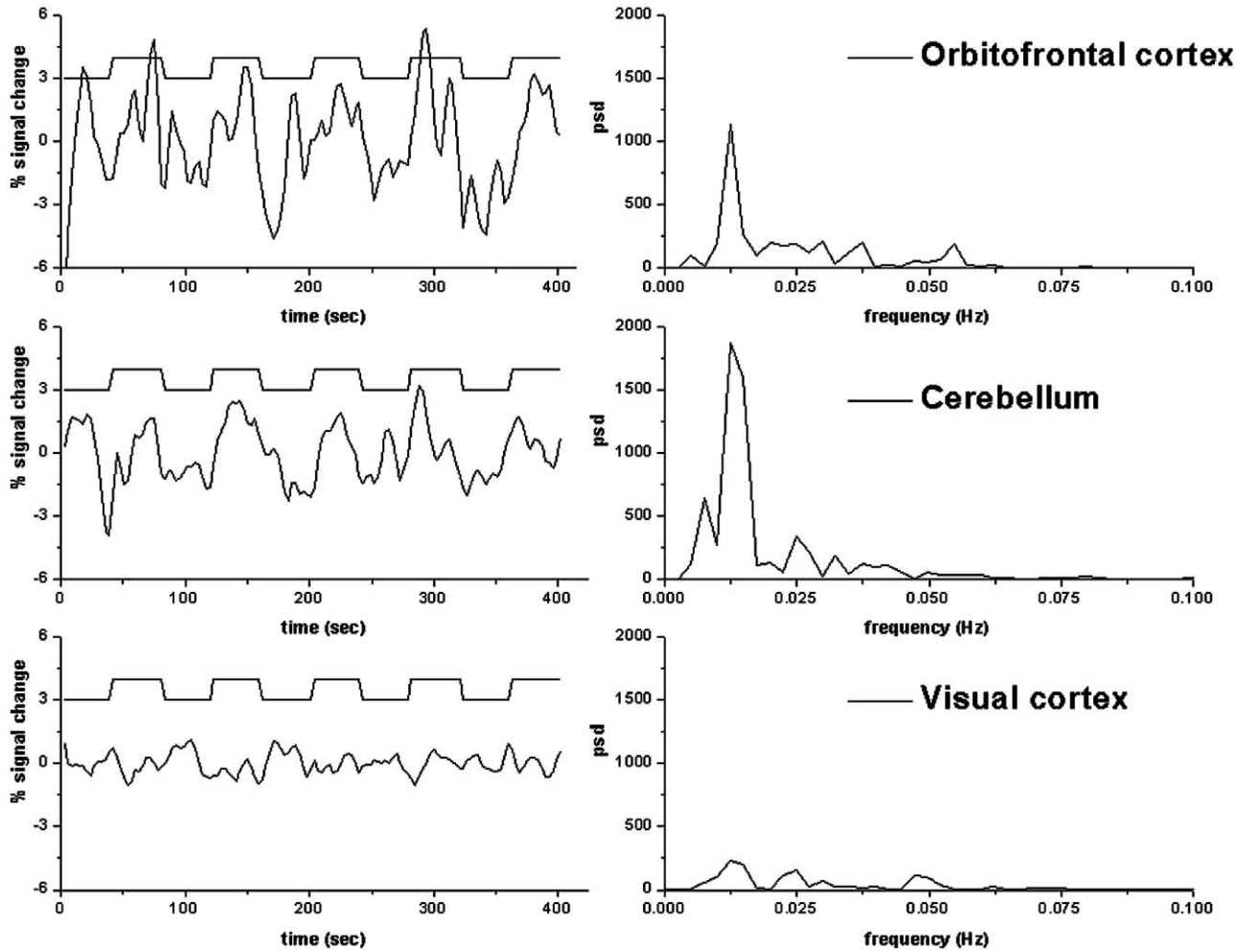

Fig. 2. Time series (left column) and associated power spectral densities (psd, right column) for fMRI data from a representative monkey in one of the olfaction experiments. Data are presented for voxels selected from orbitofrontal cortex (top row), cerebellum (middle row), and visual cortex as a control (bottom row). The off–on experimental design depicted by the top line in each of the left panels illustrates 40 s of clean air exposure alternated with 40 s of odorant presentation. The psds (right column) show clear peaks at the task frequency of 0.0125 Hz (= 1/80).

tion" in the sedated monkey brain. At the same threshold used to examine activation as noted above ($P < 0.001$, five-voxel extent), odorant-induced deactivation was not detected anywhere in the brain.

Odor intensity effects

Activations evoked by the three different odorant concentrations scored separately for each monkey did not differ significantly, as indicated by Wilcoxon's tests ($P > 0.05$) for the percentage of voxels activated above threshold in each ROI. The percentage of activated voxels did not differ across the three odorant concentrations regardless of whether bilateral ROIs were subdivided into right and left unilateral hemispheric subregions. Similar results were found for the percentage of signal change in each ROI. Subsequent ROI-based analyses were therefore conducted with data for each monkey averaged across the odorant concentrations.

Regional differences

Signal changes of 0.7% were observed, on average, in the orbitofrontal cortex and the cerebellum. These changes were significantly greater than chance levels of activation ($P < 0.05$, two-tailed). The percentage of signal change in the piriform cortex, but not the hippocampus nor visual cortex, likewise tended to exceed chance levels ($P < 0.10$, two-tailed), as depicted in Fig. 3.

Discussion

In sedated squirrel monkeys, a distributed network of activation was detected in the orbitofrontal cortex, cerebellum, and, to a lesser extent, the piriform cortex in response to three different odorant concentrations. The time course of activation consistently followed the on–off pattern of odorant presentation as measured by time series and power spectral density analysis. These findings in sedated mon-

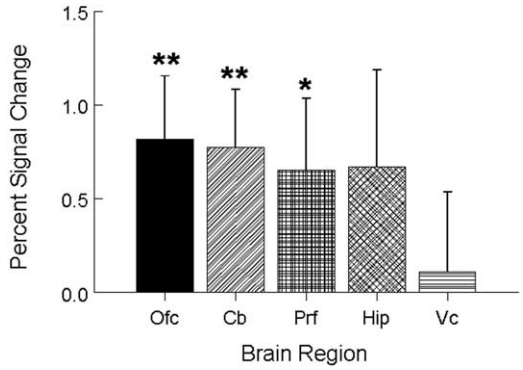

Fig. 3. Percentages of signal change in bilateral brain regions induced by olfactory processing in monkeys (mean ± SEM). Measures that differ significantly from chance are depicted by double ($P < 0.05$) or a single ($P < 0.10$) asterisk. Ofc, orbitofrontal cortex; Cb, cerebellum; Prf, piriform cortex; Hip, hippocampus; Vc, visual cortex.

keys correspond with those reported in studies of olfaction in alert conscious humans (Doty, 2001; Zald and Pardo, 2000). Comparable patterns of BOLD activation suggest that brain substrates subserving olfaction are tightly coupled such that stimulation in sedated and nonsedated states triggers activation of the entire distributed olfactory neural network.

The observed signal changes in monkeys compare favorably with human data. Block-design fMRI studies of humans using $3.2 \times 3.2 \times 4.5$ mm^3 voxels generally find signal changes of 5% or less. Assuming that BOLD signal decreases linearly with reduced voxel volumes, one could expect signal changes on the order of 0.2% or less based on the $1.25 \times 1.25 \times 1.2$ mm^3 voxel resolution used in our study. The signal changes observed in the orbitofrontal cortex and cerebellum were nearly three times greater, indicating that these activations are strong and remarkably robust.

Animal studies have characterized the involvement of primary olfactory structures, i.e., the olfactory bulb, piriform cortex, and entorhinal cortex, as well as accessory brain regions, including the orbitofrontal cortex, in olfactory processing (Pautler and Koretsky, 2002; Shipley and Ennis, 1996). Consistent with these findings, we found varying degrees of activation in the piriform and orbitofrontal cortices. Moderate activation in the piriform cortex agrees with human neuroimaging studies (Sobel et al., 2000; Zatorre et al., 1992), as well as studies of animals (Shipley and Ennis, 1996). Extensive projections from the primary olfactory cortex and thalamus to the orbitofrontal cortex are likewise consistent with our findings from fMRI studies of monkeys (Carmichael et al., 1994; Carmichael and Price, 1996; Ray and Price, 1993; Yarita et al., 1980). Although the inclusion of the entorhinal cortex as part of the primary olfactory cortex has been well established (de Olmos et al., 1978), widespread variation in the extent of activation for this region has been reported in human neuroimaging studies of olfaction (Zald and Pardo, 2000). Variability may be due to dropout artifacts (Ojemann et al., 1997) like those that obliterated BOLD signal activation for this region in monkeys.

Imaging studies indicate that additional brain regions, including the cerebellum, are intimately involved in human olfactory processing (Sobel et al., 1998a, 1998b; Yousem et al., 1997). Cerebellar activation has been hypothesized to reflect both sniffing and odorant detection (Sobel et al., 1998a). Insofar as the sniff reflex is preserved in sedated states (Tomori et al., 1998), cerebellar activation in sedated squirrel monkeys may be due to reflexive sniffing and/or odorant detection. Studies designed to monitor and compare respiration during odorant versus clean air presentations are needed to determine if cerebellar activation is related to sniffing or odorant detection in sedated monkeys. In either case, our findings provide novel support for the hypothesis that the cerebellum plays an important role in sensory acquisition (Gao et al., 1996).

Despite a 100-fold difference between the high and low odorant concentrations presented in our experiments with monkeys, significant differences were not discerned in the extent of BOLD activation in any anatomically defined ROI. These findings are consistent with human neuroimaging studies of olfaction that have failed to show odor intensity effects in any of the ROIs we examined in monkeys. An earlier study of eight healthy men noted a trend ($P < 0.10$, one-tailed) toward greater thalamic activation in response to a putative human pheromone presented at high versus low concentrations (Sobel et al., 1999). No dose-dependent response patterns were detected in any of 11 other regions that demonstrated activation in more than a single human subject. On the other hand, an event-related fMRI study recently reported that amygdala activation in humans reflects variation in odorant concentration or intensity (Anderson et al., 2003). In addition to including the amygdala in future imaging studies of olfaction, we plan to improve our ROI-based approach by relying on the activations discerned here to demarcate a robust *a priori* set of functional ROIs. This approach should achieve far greater anatomical precision for testing odor intensity effects in studies of monkeys.

Our failure to find odor concentration effects in monkey orbitofrontal cortex is consistent with a study of humans (Anderson et al., 2003) that reported activation in this region is associated with odor valence (i.e., pleasant versus unpleasant) independently of intensity. Our study of monkeys used unpleasant acetic acid odors that in strong doses can stimulate the trigeminal nerve in the nasal mucosa (Doty, 1995, 2001). Trigeminal nerve stimulation effects on brain activation are not clearly known. Nevertheless, the ability to detect BOLD activation in monkey orbitofrontal cortex at a magnitude exceeding that found in humans provides important opportunities to extend our understanding of odor valence processing and related aspects of olfaction.

At 3T, without contrast agents, and using conventional imaging techniques, it is possible to detect robust activation in monkey brain regions known to be involved in olfactory processing in humans. Moreover, it is possible to image the

whole brain at high resolution with isotropic voxels of 1.25 × 1.25 × 1.2 mm. To maintain isotropy at this level of resolution across the brain required the use of 24 contiguous image slices, the largest number in any fMRI study of monkeys published to date. Multiple repeated on–off cycles of stimulus presentation allowed us to detect robust activation similar to that seen in previous fMRI studies of visual processing in monkeys (Logothetis et al., 2002; Rainer et al., 2001; Sereno et al., 2002; Tolias et al., 2001). Our use of standard imaging techniques and a 3T scanner facilitate direct comparisons with human fMRI data and therefore represent an ideal methodology for comparative functional studies of olfactory brain systems in primates. Although some fMRI studies of monkeys have relied on 1.5T scanners (Dubowitz et al., 1998; Hayashi et al., 1999; Nakahara et al., 2002; Stefanacci et al., 1998; Vanduffel et al., 2001), significant improvements in signal intensity (25–75%) are evident at 3T field strength (Krasnow et al., 2003). 3T scanners are increasingly common in human neuroimaging research, and these scanners are especially well suited for comparative primate brain research.

A final aspect of this study that warrants comment concerns the absence of odorant-induced "deactivation" in the sedated monkey brain. At a minimum, this finding indicates that odorant-induced patterns of activation in our study do not simply reflect "random noise." A more intriguing possibility concerns deactivation as an index of default-mode network activity in the resting brain (Greicius et al., 2002). Functional brain imaging has traditionally focused on regions that reliably show task-related increases in neural activity. Nevertheless, there are several brain regions in which neural activity is greater during baseline "resting" epochs than during the experimental task. Such task-related decreases in activation are referred to as "deactivation," and certain regions consistently demonstrate deactivation across a broad range of cognitive tasks (Shulman et al., 1997). Raichle and colleagues (2001) have suggested that certain of these regions constitute an organized "default-mode network" whose activity is ongoing during rest or simple tasks and suspended during performance of externally cued tasks.

Based on these intriguing observations in humans, there are two alternative reasons sedated monkeys fail to show externally cued deactivations. One possibility is that sedation selectively switches off the default-mode network. Support for this hypothesis comes from a regional cerebral blood flow study in humans indicating that regions that are commonly deactivated by externally cued tasks also show decreases in activity in proportion to waning consciousness induced during sedation (Fiset et al., 1999). Alternatively, it is possible that humans and nonhuman primates differ in terms of having an organized default-mode network whose activity is suspended during performance of externally cued tasks. At present, very little information is available on this important topic. In any case, both of these possibilities offer testable hypotheses, the answers to which will most likely provide useful insights into human and nonhuman cognitive processes and perhaps consciousness itself.

Acknowledgments

We thank Ben Krasnow and Eric Schmitt for assistance with data analysis; Anne Sawyer-Glover, Gary Glover, and Marc Alley for invaluable technical support; and two anonymous reviewers for helpful comments. This work was funded by the Pritzker Network, the Norris Fund, and NIH Grants HD40761, MH64230, MH47573, MH050604, and MH062131.

References

Anderson, A.K., Christoff, K., Stappen, I., Panitz, D., Ghahremani, D.G., Glover, G., Gabrieli, J.D., Sobel, N., 2003. Dissociated neural representations of intensity and valence in human olfaction. Nat. Neurosci. 6 (2), 196–202.

Carmichael, S.T., Clugnet, M.C., Price, J.L., 1994. Central olfactory connections in the macaque monkey. J. Comp. Neurol. 346 (3), 403–434.

Carmichael, S.T., Price, J.L., 1996. Connectional networks within the orbital and medial prefrontal cortex of macaque monkeys. J. Comp. Neurol. 371 (2), 179–207.

de Olmos, J., Hardy, H., Heimer, L., 1978. The afferent connections of the main and the accessory olfactory bulb formations in the rat: an experimental HRP-study. J. Comp. Neurol. 181 (2), 213–244.

Doty, R.L., 1995. Intranasal trigeminal chemoreception: anatomy, physiology, and psychophysics, in: Doty, R.L. (Ed.), Handbook of Olfaction and Gustation. Dekker, New York.

Doty, R.L., 2001. Olfaction. Annu. Rev. Psychol. 52, 423–452.

Dubowitz, D.J., Chen, D.Y., Atkinson, D.J., Grieve, K.L., Gillikin, B., Bradley Jr., W.G., Andersen, R.A., 1998. Functional magnetic resonance imaging in macaque cortex. NeuroReport 9 (10), 2213–2218.

Ferris, C.F., Snowdon, C.T., King, J.A., Duong, T.Q., Ziegler, T.E., Ugurbil, K., Ludwig, R., Schultz-Darken, N.J., Wu, Z., Olson, D.P., Sullivan Jr, J.M., Tannenbaum, P.L., Vaughan, J.T., 2001. Functional imaging of brain activity in conscious monkeys responding to sexually arousing cues. NeuroReport 12 (10), 2231–2236.

Fiset, P., Paus, T., Daloze, T., Plourde, G., Meuret, P., Bonhomme, V., Hajj-Ali, N., Backman, S.B., Evans, A.C., 1999. Brain mechanisms of propofol-induced loss of consciousness in humans: a positron emission tomographic study. J. Neurosci. 19 (13), 5506–5513.

Friston, K.J., Holmes, A.P., Worsler, K., Poline, J.-P., Frith, C.D., Frackowiak, R.S.J., 1995. Statistical parametric maps in functional imaging: A general linear approach. Hum. Brain Mapp. 2, 189–210.

Gao, J.H., Parsons, L.M., Bower, J.M., Xiong, J., Li, J., Fox, P.T., 1996. Cerebellum implicated in sensory acquisition and discrimination rather than motor control. Science 272 (5261), 545–547.

Gergen, J.A., MacLean, P.D., 1962. A Stereotaxic Atlas of the Squirrel Monkey's Brain, Vol. 933, U.S. Department of Health, Education, and Welfare, Bethesda, MD.

Greicius, M.D., Krasnow, B., Reiss, A.L., Menon, V., 2003. Functional connectivity in the resting brain: a network analysis of the default mode hypothesis. Proc. Natl. Acad. Sci. USA. 100 (1), 253–258.

Hayashi, T., Konishi, S., Hasegawa, I., Miyashita, Y., 1999. Short communication: mapping of somatosensory cortices with functional magnetic resonance imaging in anaesthetized macaque monkeys. Eur. J. Neurosci. 11 (12), 4451–4456.

Hayes, M.H., 1996. Statistical Digital Signal Processing and Modeling. Wiley, New York.

Hildebrand, J.G., Shepherd, G.M., 1997. Mechanisms of olfactory discrimination: converging evidence for common principles across phyla. Annu. Rev. Neurosci. 20, 595–631.

Kauer, J.S., White, J., 2001. Imaging and coding in the olfactory system. Annu. Rev. Neurosci. 24, 963–979.

Krasnow, B., Tamm, L., Yang, T.T., Greicius, M., Glover, G.H., Reiss, A.L., Menon, V., 2003. Comparison of fMRI activation at 3T and 1.5T

during perceptual, cognitive and affective processing. Neuroimage 18 (4), 813–1013.
Lahti, K.M., Ferris, C.F., Li, F., Sotak, C.H., King, J.A., 1999. Comparison of evoked cortical activity in conscious and propofol- anesthetized rats using functional MRI. Magn. Reson. Med. 41 (2), 412–416.
Leite, F.P., Tsao, D., Vanduffel, W., Fize, D., Sasaki, Y., Wald, L.L., Dale, A.M., Kwong, K.K., Orban, G.A., Rosen, B.R., Tootell, R.B., Mandeville, J.B., 2002. Repeated fMRI using iron oxide contrast agent in awake, behaving macaques at 3 Tesla. Neuroimage 16 (2), 283–294.
Leopold, D.A., Plettenberg, H.K., Logothetis, N.K., 2002. Visual processing in the ketamine-anesthetized monkey. Optokinetic and blood oxygenation level-dependent responses. Exp. Brain Res. 143 (3), 359–372.
Logothetis, N., Merkle, H., Augath, M., Trinath, T., Ugurbil, K., 2002. Ultra high-resolution fMRI in monkeys with implanted RF coils. Neuron 35 (2), 227–242.
Logothetis, N.K., Guggenberger, H., Peled, S., Pauls, J., 1999. Functional imaging of the monkey brain. Nat. Neurosci. 2 (6), 555–562.
Lovibond, P.F., Shanks, D.R., 2002. The role of awareness in Pavlovian conditioning: empirical evidence and theoretical implications. J. Exp. Psychol. Anim. Behav. Process 28 (1), 3–26.
Lyons, D.M., Afarian, H., Schatzberg, A.F., Sawyer-Glover, A., Moseley, M.E., 2002. Experience-dependent asymmetric variation in primate prefrontal morphology. Behav. Brain Res. 136 (1), 51–59.
Lyons, D.M., Yang, C., Sawyer-Glover, A.M., Moseley, M.E., Schatzberg, A.F., 2001. Early life stress and inherited variation in monkey hippocampal volumes. Arch. Gen. Psychiatry 58 (12), 1145–1151.
Malaspina, D., Perera, G.M., Lignelli, A., Marshall, R.S., Esser, P.D., Storer, S., Furman, V., Wray, A.D., Coleman, E., Gorman, J.M., Van Heertum, R.L., 1998. SPECT imaging of odor identification in schizophrenia. Psychiatry Res. 82 (1), 53–61.
Martin, R.F.a.B.D.M., 2000. Primate Brain Maps: Structure of the Macaque Brain. Elsevier, Amsterdam.
Moonen, C.T.W., Bandettini, P.A., 1999. Functional MRI, Vol. xii. Springer-Verlag, Berlin.
Nakahara, K., Hayashi, T., Konishi, S., Miyashita, Y., 2002. Functional MRI of macaque monkeys performing a cognitive set-shifting task. Science 295 (5559), 1532–1536.
Ojemann, J.G., Akbudak, E., Snyder, A.Z., McKinstry, R.C., Raichle, M.E., Conturo, T.E., 1997. Anatomic localization and quantitative analysis of gradient refocused echo-planar fMRI susceptibility artifacts. Neuroimage 6 (3), 156–167.
Pautler, R.G., Koretsky, A.P., 2002. Tracing odor-induced activation in the olfactory bulbs of mice using manganese-enhanced magnetic resonance imaging. Neuroimage 16 (2), 441–448.
Plettenberg, A., Albrecht, D., Lorenzen, T., Meyer, T., Arndt, R., Stoehr, A., 2002. Monitoring of endogenous interferon-alpha and human herpesvirus 8 in HIV-infected patients with Kaposi's sarcoma. Eur. J. Med. Res. 7 (1), 19–24.
Raichle, M.E., MacLeod, A.M., Snyder, A.Z., Powers, W.J., Gusnard, D.A., Shulman, G.L., 2001. A default mode of brain function. Proc. Natl. Acad. Sci. USA 98 (2), 676–682.
Rainer, G., Augath, M., Trinath, T., Logothetis, N.K., 2001. Nonmonotonic noise tuning of BOLD fMRI signal to natural images in the visual cortex of the anesthetized monkey. Curr. Biol. 11 (11), 846–854.
Ray, J.P., Price, J.L., 1993. The organization of projections from the mediodorsal nucleus of the thalamus to orbital and medial prefrontal cortex in macaque monkeys. J. Comp. Neurol. 337 (1), 1–31.
Rorden, C., Brett, M., 2000. Stereotaxic display of brain lesions. Behav. Neurol. 12 (4), 191–200.
Semendeferi, K., Damasio, H., 2000. The brain and its main anatomical subdivisions in living hominoids using magnetic resonance imaging. J. Hum. Evol. 38 (2), 317–332.
Sereno, M.E., Trinath, T., Augath, M., Logothetis, N.K., 2002. Three-dimensional shape representation in monkey cortex. Neuron 33 (4), 635–652.
Shipley, M.T., Ennis, M., 1996. Functional organization of olfactory system. J. Neurobiol. 30 (1), 123–176.
Shulman, G.L., Fiez, J.A., Corbetta, M., Buckner, R.L., Miezin, F.M., Raichle, M.E., Petersen, S.E., 1997. Common blood flow changes across visual tasks: II. Decreases in cerebral cortex. J. Cogn. Neurosci. 9, 648–663.
Skudlarski, P., Constable, R.T., Gore, J.C., 1999. ROC analysis of statistical methods used in functional MRI: individual subjects. Neuroimage 9 (3), 311–329.
Sobel, N., Prabhakaran, V., Desmond, J.E., Glover, G.H., Goode, R.L., Sullivan, E.V., Gabrieli, J.D., 1998a. Sniffing and smelling: separate subsystems in the human olfactory cortex. Nature 392 (6673), 282–286.
Sobel, N., Prabhakaran, V., Desmond, J.E., Glover, G.H., Sullivan, E.V., Gabrieli, J.D., 1997. A method for functional magnetic resonance imaging of olfaction. J. Neurosci. Methods 78 (1-2), 115–123.
Sobel, N., Prabhakaran, V., Hartley, C.A., Desmond, J.E., Glover, G.H., Sullivan, E.V., Gabrieli, J.D., 1999. Blind smell: brain activation induced by an undetected air-borne chemical. Brain 122 (Pt. 2), 209–217.
Sobel, N., Prabhakaran, V., Hartley, C.A., Desmond, J.E., Zhao, Z., Glover, G.H., Gabrieli, J.D., Sullivan, E.V., 1998b. Odorant-induced and sniff-induced activation in the cerebellum of the human. J. Neurosci. 18 (21), 8990–9001.
Sobel, N., Prabhakaran, V., Zhao, Z., Desmond, J.E., Glover, G.H., Sullivan, E.V., Gabrieli, J.D., 2000. Time course of odorant-induced activation in the human primary olfactory cortex. J. Neurophysiol. 83 (1), 537–551.
Sparks, D.L., Corssen, G., Sides, J., Black, J., Kholeif, A., 1973. Ketamine-induced anesthesia: neural mechanisms in the Rhesus monkey. Anesth. Analg. 52 (2), 288–297.
Stefanacci, L., Reber, P., Costanza, J., Wong, E., Buxton, R., Zola, S., Squire, L., Albright, T., 1998. fMRI of monkey visual cortex. Neuron 20 (6), 1051–1057.
Tolias, A.S., Smirnakis, S.M., Augath, M.A., Trinath, T., Logothetis, N.K., 2001. Motion processing in the macaque: revisited with functional magnetic resonance imaging. J. Neurosci. 21 (21), 8594–8601.
Tomori, Z., Benacka, R., Donic, V., 1998. Mechanisms and clinicophysiological implications of the sniff- and gasp-like aspiration reflex. Respir. Physiol. 114 (1), 83–98.
Vanduffel, W., Fize, D., Mandeville, J.B., Nelissen, K., Van Hecke, P., Rosen, B.R., Tootell, R.B., Orban, G.A., 2001. Visual motion processing investigated using contrast agent-enhanced fMRI in awake behaving monkeys. Neuron 32 (4), 565–577.
West, S.E., Doty, R.L., 1995. Influence of epilepsy and temporal lobe resection on olfactory function. Epilepsia 36 (6), 531–542.
Xu, F., Kida, I., Hyder, F., Shulman, R.G., 2000. Assessment and discrimination of odor stimuli in rat olfactory bulb by dynamic functional MRI. Proc. Natl. Acad. Sci. USA 97 (19), 10601–10606.
Yang, X., Renken, R., Hyder, F., Siddeek, M., Greer, C.A., Shepherd, G.M., Shulman, R.G., 1998. Dynamic mapping at the laminar level of odor-elicited responses in rat olfactory bulb by functional MRI. Proc. Natl. Acad. Sci. USA 95 (13), 7715–7720.
Yarita, H., Iino, M., Tanabe, T., Kogure, S., Takagi, S.F., 1980. A transthalamic olfactory pathway to orbitofrontal cortex in the monkey. J. Neurophysiol. 43 (1), 69–85.
Yousem, D.M., Williams, S.C., Howard, R.O., Andrew, C., Simmons, A., Allin, M., Geckle, R.J., Suskind, D., Bullmore, E.T., Brammer, M.J., Doty, R.L., 1997. Functional MR imaging during odor stimulation: preliminary data. Radiology 204 (3), 833–838.
Zald, D.H., Pardo, J.V., 2000. Functional neuroimaging of the olfactory system in humans. Int. J. Psychophysiol. 36 (2), 165–181.
Zatorre, R.J., Jones-Gotman, M., 1991. Human olfactory discrimination after unilateral frontal or temporal lobectomy. Brain 114 (Pt. 1A), 71–84.
Zatorre, R.J., Jones-Gotman, M., Evans, A.C., Meyer, E., 1992. Functional localization and lateralization of human olfactory cortex. Nature 360 (6402), 339–340.